CRYSTAL GROWTH & DESIGN
2009
VOL. 9, NO. 5
2324–2328

Single-Crystalline Anatase TiO_2 Dous Assembled Micro-Sphere and Their Photocatalytic Activity

Xiaoye Hu,*,† Tianci Zhang,† Zhen Jin,† Suzhen Huang,‡ Ming Fang,† Yucheng Wu,† and Lide Zhang*,†

Key Laboratory of Materials Physics, and Anhui Key Laboratory of Nanomaterials and Nanostructures, Institute of Solid State Physics, Chinese Academy of Sciences, Hefei 230031, P. R. China, and Institute of Plasma Physics, Chinese Academy of Sciences, Hefei 230031, P. R. China

Received October 21, 2008; Revised Manuscript Received January 10, 2009

ABSTRACT: Using anodized TiO_2 nanotubes as the starting materials, unique structural single-crystalline anatase TiO_2 dous assembled microspheres are fabricated by a hydrothermal method. The single-crystalline anatase TiO_2 dou is formed through the transformation of a TiO_2 nanotube, which is formed through a complex process including the expansion of the nanotube, dissolution−recrystallization, and recombination. The opening and hollow structural dou exposes one {001} face and eight {101} faces, which displays excellent photocatalytic activity. And it is also envisaged to be of high promise for many other potential applications. The approach might be exploited for the synthesis of single-crystalline nanomaterials with special morphologies.

1. Introduction

As increasing interest has been invested in anatase titanium dioxide (TiO_2), many researchers have focused their attention on the controllable fabrication of anatase nano-TiO_2, since the large surface area widely is considered to be useful to improve their potential properties.[1−15] It should be also noted that, besides the high surface area, the crystallinity and exposed facet of TiO_2 are two other important factors influencing the properties. That is to say, by unilaterally increasing the surface area, the properties of TiO_2 are still relatively confined due to their poor crystallinity and less reactive surfaces. Therefore, in order to considerably improve the properties, it would be very necessary to synthesize single-crystalline anatase TiO_2, especially those with special morphologies, high surface area, and many reactive surfaces. Unfortunately, the fabrication of single-crystalline anatase TiO_2 is difficult, because anatase TiO_2 is a thermodynamically metastable phase. Up to now, the typical results are some anatase TiO_2 single crystals with octahedral bipyramid and truncated octahedral bipyramid structure fabricated by controlling the growth rate of {001} and {101} faces.[16−19] For a practical application, it might be more desirable to obtain single-crystalline anatase TiO_2 with special morphologies, such as hollow and opening geometrical structures. However, by using traditional starting materials and synthesis methods, it is very difficult to fabricate anatase TiO_2 single crystals with controllable structures.

Herein, we report a controllable fabrication of single-crystalline anatase TiO_2. Open hollow single-crystalline anatase TiO_2 dous (A "dou" is a kind of chinese peck with an open hollow truncated pyramid structure) assembled microspheres are first synthesized using TiO_2 nanotubes as starting materials under hydrogen peroxide (H_2O_2) and hydrofluoric acid (HF) conditions via hydrothermal reacting. Each single dou exposes one {001} face with high surface energy and eight {101} faces with relatively low surface energy.[20−22] As based on the calculation, we confirmed that these microspheres expose about 20−40% highly reactive (001) faces, which can improve the properties of TiO_2 for application in sensing, dye-sensitized solar cells, H_2 preparation from water, organic pollutant treatment in the environment, etc. Moreover, detailed structural analysis would give vital clues to understand the growth mechanism of the nanostructure. And the designed synthesis method might be exploited to synthesize single-crystalline nanomaterials with special morphologies for practical applications.

2. Experimental Section

The synthesis of the single-crystalline anatase TiO_2 dous assembled microspheres was carried out in two steps. First, TiO_2 nanotubes were fabricated by anodizing the pure Ti sheet as described previously.[23,24] In brief, the high-purity (99.999%) titanium plate was anodized in mixing electrolyte of ethylene glycol and hydrofluoric acid (0.2 M) for 10 h. The anodizing voltage was 100 V and the temperature of the electrolyte was kept at 15 °C. Subsequently, the sample was rinsed with deionized water and dried. Then, the as-fabricated TiO_2 nanotube array was separated from the Ti sheet. After that, the as-fabricated TiO_2 nanotubes (40 mg) were added to a 50 mL autoclave with hydrogen peroxide (with a concentration of 30%) and HF acid (0.05−0.15 mL with concentration of 40%). After hydrothermal reaction at 180 °C for 5 h, white powders were obtained by centrifugation. Finally, the products were dried in the air and annealed in oxygen for 2 h at 450 °C to remove the residual F from the sample.

The morphologies of the samples were examined by field-emission scanning electron microscopy (FE-SEM; FEI Sirion-200) and high-resolution transmission electron microscopy (HRTEM; JEM-2010). Moreover, the crystal structure of the samples was determined by Raman spectroscopy with an Ar + laser excitation (514.5 nm). And the photocatalytic activity of the samples was evaluated based upon the removal of methylene blue (MB) dye in the aqueous solution. During the process of photocatalysis experiments, the changes of the concentration of MB were monitored by UV−vis spectroscopy.

3. Results and Discussion

3.1. Structure and Morphology. Figure 1 shows the top-surface SEM images of TiO_2 nanotubes. The as-fabricated TiO_2 nanotubes are properly clean without any remnants. And the inner and outer diameters are around 96 and 170 nm, respectively, as described in our previous work.[24] Figure 2a,b shows the SEM images of anatase TiO_2 microspheres. It can be clearly seen that the product contains lots of microspheres with a diameter of about 2.5 μm, which is assembled by many dous.

* To whom correspondence should be addressed: E-mail: hxy821982@issp.ac.cn (X.Y.H.), ldzhang@issp.ac.cn (L.D.Z.); fax: (+86) 551-559-1434.
† Key Laboratory of Materials Physics, and Anhui Key Laboratory of Nanomaterials and Nanostructures, Institute of Solid State Physics, Chinese Academy of Sciences.
‡ Institute of Plasma Physics, Chinese Academy of Sciences.

10.1021/cg801181y CCC: $40.75
Published on Web 02/27/2009

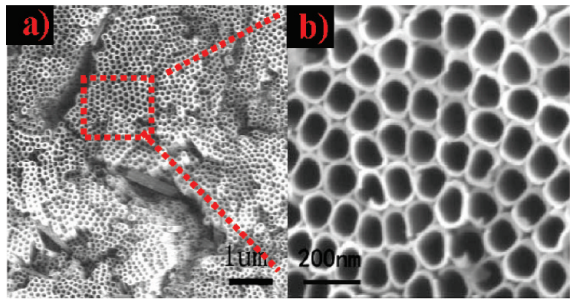

Figure 1. (a) SEM images of TiO_2 nanotubes. (b) The enlarged image of panel a.

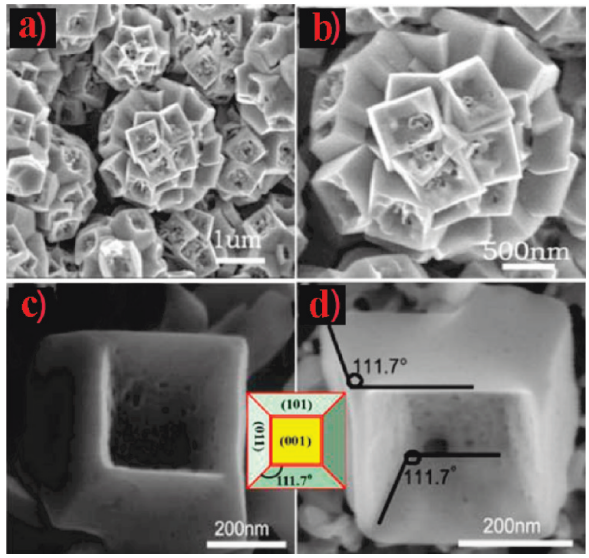

Figure 2. SEM images of the anatase TiO_2 microspheres and the unit TiO_2 dou. (a) The microspheres synthesized with 40 mg of TiO_2 nanotubes under the H_2O_2 (30%) and 0.05 mL of HF (40%) at 180 °C for 5 h. (b) The enlarged image of panel a. (c and d) The single TiO_2 dou was obtained from the microspheres by ultrasonic treatment. The inset is a geometrical model of the single dou.

In order to investigate the structure of the single TiO_2 dou, the as-fabricated samples were treated using an ultrasonic oscillator to obtain the single dou, as shown in Figure 2c,d. From Figure 2d, the interfacial angles between the top and underside two parallel faces (flat square planes) and other surrounding isosceles trapezoidal faces are about 111.7°, respectively. The inner bottom square plane of the dou is porous. Considering the calculated value,[16,25] the top and bottom square planes of the dou should be {001} faces and the four isosceles trapezoidal surfaces are {101} faces of anatase TiO_2 single crystals. It is very clear that the inside four isosceles trapezoidal surfaces are, respectively, parallel to the corresponding outside {101} faces. Hence, the porous facet can be predicatively assigned as (001), which is also confirmed by the images of the high-resolution transmission electron microscopy (HRTEM), as shown in Figure 3. Unfortunately, we did not observe a perfect single dou under the TEM observation due to ultrasonic treatment. Nevertheless, we are able to observe the dou-like structure of the sample from Figure 3b. The selected-area electron diffraction (SAED) pattern confirms that the single dou has a single-crystalline nature (Figure 3c). Furthermore, the lattice image (Figure 3d) clearly reveals that the distance between the adjacent lattice fringes are assigned to the (200) interplanar distance of anatase TiO_2, which is $d_{200} = 0.189$ nm. As a further confirmation, this anatase

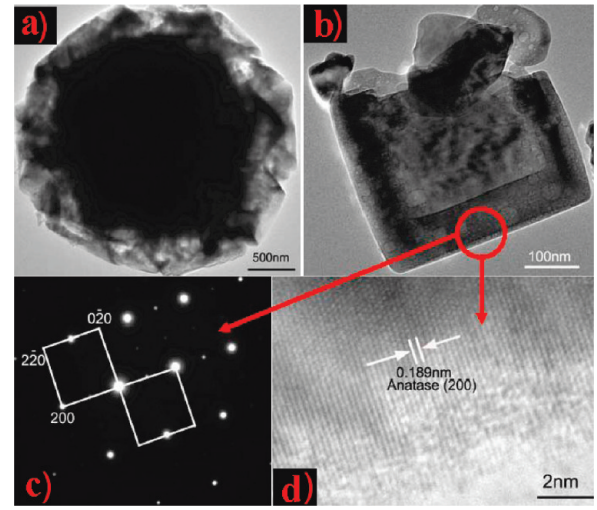

Figure 3. TEM images of microsphere and the crystalline phase of the unit TiO_2 dou. (a and b) TEM images corresponding to the sample in Figure 1, panels b and d, respectively. (c and d) The selected-area electron diffraction pattern and the lattice image of the single TiO_2 dou from the microsphere, respectively. The electron diffraction pattern was recorded perpendicular to the (001) plane.

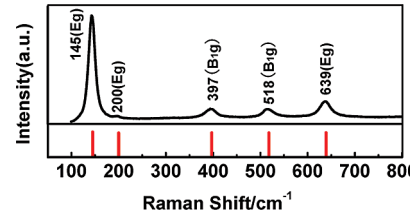

Figure 4. The Raman spectrum of the as-fabricated sample. The straight lines at the bottom perpendicular to the X axis show the position of standard anatase TiO_2.

crystallographic phase of the sample is also clearly indicated by the Raman result (Figure 4). The Raman spectrum shows five very sharp peaks centered at 145, 200, 397, 518, and 639 cm^{-1}, which can be attributed to the Raman-active modes of anatase phase with the symmetries of Eg, Eg, B1g, B1g, and Eg, respectively.[17,26] All this evidence confirms that the dou is anatase TiO_2 single crystal.

3.2. The Growth Mechanism. To further explore the transformation process of the TiO_2 nanotube to the dous, we investigated the experimental results in detail at different reaction times. Figure 5 displays a series of evolutional TEM images together with the corresponding simulated three-dimensional structures. Deduced from these experimental data, the transformation from nanotubes to the dous, and to the microspheres is a "dissolution−recrystallization" process.[27−30] The process could be summarized in three processes: (1) the TiO_2 nanotubes inflate and fracture; (2) the cylindrical walls of TiO_2 nanotubes transform into trapezoidal faces, forming the dous; (3) dous assemble into the microspheres.

During the process of hydrothermal reacting, the wall of the anodized TiO_2 nanotube is gradually dissolved by HF solution to form TiF_4, which causes thinning of the nanotube wall. On the other hand, the oxygen isolating from the H_2O_2 inside the nanotube is not able to be quickly released from the mouth of the nanotube, thus enhancing the pressure inside the nanotubes. When the hydrothermal reaction runs to 90 min, the wall of TiO_2 nanotube is thin enough. In this case, the high oxygen pressure inside the nanotube causes the nanotube to bulge

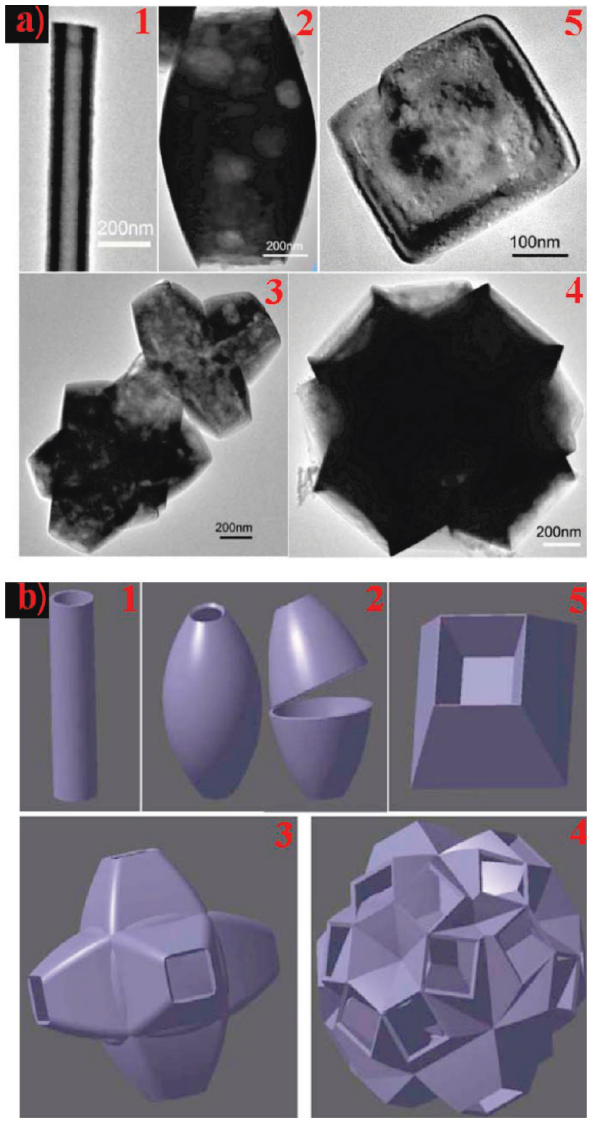

Figure 5. The process of transformation from the TiO_2 nanotube to the dou, then to the microsphere. (a) TEM images of these samples obtained at different reaction times and (b) the corresponding simulated three-dimensional structural images. (1) The primitive TiO_2 nanotube, (2) 90 min, (3) 150 min, (4) 240 min, and (5) the unit truncated pyramid from the sample shown in (4).

outward to form many drum-like hollow columns, with the rapid stress increasing, resulting in the fracture of the TiO_2 nanotube. And the fracture action would instantaneously occur throughout the whole TiO_2 nanotube, which causes the nanotube to be cut down to several parts, forming the truncated cones and dumbbell-shaped structures. The dumbbell-shaped structures are then fractured to form the cones again. This process is shown in Figures 5a-2, 5b-2 and 6-2, 6-3, 6-4, and 6-5.

As the dissolution process of the wall of the TiO_2 nanotube continues, the concentration of HF inside the nanotube is lowered more quickly than that on the outside of the nanotube, because the HF inside the nanotube is difficult to exchange with that outside the nanotubes resulting from the release of oxygen from the mouth of nanotube. When the concentration of HF inside the nanotube decreases to a certain value, TiF_4 presents a hydrolytic reaction to transform into TiO_2, and grows along the [001] and [101] directions to form the four isosceles trapezoidal {101} surfaces on the inside wall of the nanotube (Figure 6-4). Finally, according to the oriented assembly

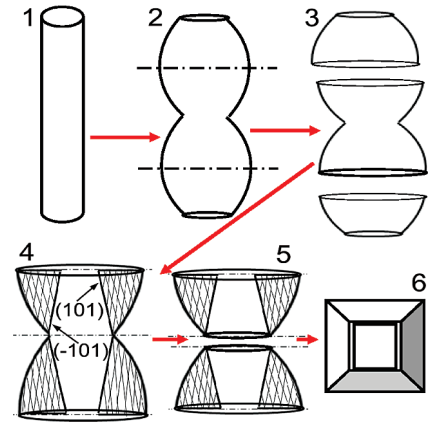

Figure 6. The fracture process of TiO_2 nanotubes. The four liny parts inside nanotube represent the growth TiO_2 from TiF_4, as shown in 4 and 5.

mechanism,[18,31,32] the four isosceles trapezoidal {101} surfaces would link each other to form the inside surface of the dou (Figure 2c,d), which would act as a template for the formation of the outside {101} surface of the dou.

In comparison with the situation inside the nanotube, the outside wall of the TiO_2 nanotube is still dissolved due to the outside HF with relatively high concentration. When the reaction is conducted for 150 min, the outside wall of anodized TiO_2 nanotube is not entirely dissolved yet. When the reaction was now stopped by cooling the autoclave to room temperature, the generated TiF_4 should present a hydrolytic reaction to transform into TiO_2 on the nondissociated outside wall of the TiO_2 nanotube, and grows to form isosceles trapezoidal surfaces, as shown in Figure 5a-3 and 5b-3. At that moment, the cylindrical walls of TiO_2 nanotube are not completely transformed into the trapezoidal surfaces; the residual cylindrical walls isolated from each other connect these trapezoidal surfaces to form the quasi-dous. And, these quasi-dous begin to self-assemble, which may be due to lots of hydroxyls produced by H_2O_2 being adsorbed on the surfaces of quasi-dous, resulting in their aggragation.[31,33,34] The self-assembling process encouraged the closure of the opening bottom of these quasi-dous, which supplied the TiO_2 source to form the (001) faces of the dous. If the hydrothermal reaction is not terminated at 150 min, the initial wall of the TiO_2nanotube should be continuously dissolved, since the solubility of many oxides are increased in water and other solutions at higher temperature and pressure.[35] As the dissolution of initial TiO_2 nanotube continues, the concentration of HF is low enough to cause the hydrolysis of TiF_4 into TiO_2 on the "template" (the template is the four isosceles trapezoidal inside surfaces of the dou formed first), and grows to form the four outside surfaces of the dou. After hydrothermal treatment for 240 min, the cylindrical walls of TiO_2 nanotubes are completely transformed into trapezoidal faces which connect to each other to form a frame according to an oriented assembly mechanism. The HRTEM image of final sample shows that the junction between the four surfaces organized so well that they assembled into a single crystal by sharing identical lattices (Figure 7). Meanwhile, it can be also seen that, after reacting 240 min, the microspheres have been almost completely formed by self-assembly of the dous (Figures 5a-4 and 5b-4). In addition, the TEM image and three-dimensional schema of the single dou also show that the (001) face inside the dou has been formed at this reaction time (Figures 5a-4 and 5b-4). When the reaction time is prolonged to 300 min, the amount of dous on the surface of the microspheres are increased, and the diameters of the

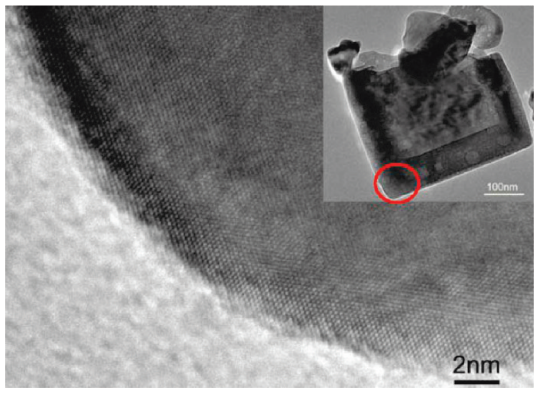

Figure 7. The adjacent side-faces lattice image of a single TiO_2 dou. The lattice image obtained from the region is marked using the schematic circle in the inset.

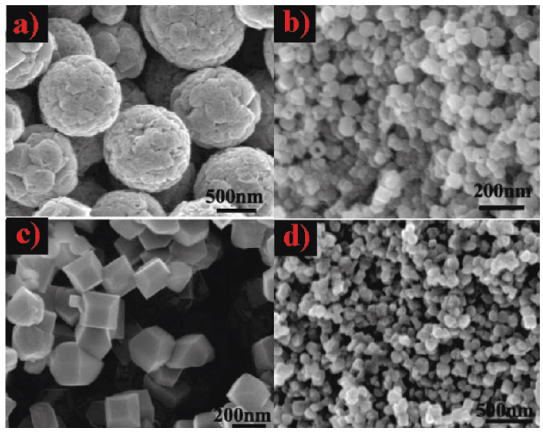

Figure 8. The SEM images of the as-fabricated samples in the solutions containing different concentrations of HF and H_2O_2. (a) 0.1 mL of HF (40%) + 45 mL of H_2O_2 (30%). (b) 0.2 mL of HF (40%) + 45 mL of H_2O_2 (30%). (c) 0.1 mL of HF (40%) + 45 mL of H_2O. (d) 0.2 mL of HF (40%) + 45 mL of H_2O.

microspheres are increased to 2.5−3 μm, forming an almost perfect microsphere (Figure 3a).

For investigation of what roles HF and H_2O_2 played in the formation process of the microspheres, the influence of the amount of HF and H_2O_2 on the morphology of the anatase crystals was examined by several experiments in different solutions. Figure 8 shows the SEM images of the as-fabricated samples from the solutions containing different concentrations of HF and H_2O_2 by hydrothermal reacting at 180 °C for 300 min. When the amount of HF increased from 0.05 to 0.1 mL, the dous on the surface of the microspheres transformed into the solid truncated bipyramids (Figure 8a). It is singular when the amount of HF was further increased to the 0.2 mL, and the ball-like structural microspheres disappeared, which were replaced by smaller nanoparticles (Figure 8b). The reason is that the high concentrations of HF completely dissolved the initial anodized TiO_2 nanotube into TiF_4 before hydrolyzation of TiF_4 inside the TiO_2 nanotube. Then, through hydrolysis, nucleation, and growth, TiF_4 transformed into a large number of anatase nanoparticles. This process is also able to be used as the interpretation of the samples synthesized in the solution containing high concentrations of HF and without H_2O_2 (Figure 8d). Under the absence of H_2O_2 conditions, when the amount of HF was 0.1 mL, only the solid truncated bipyramids were obtained (Figure 8c).

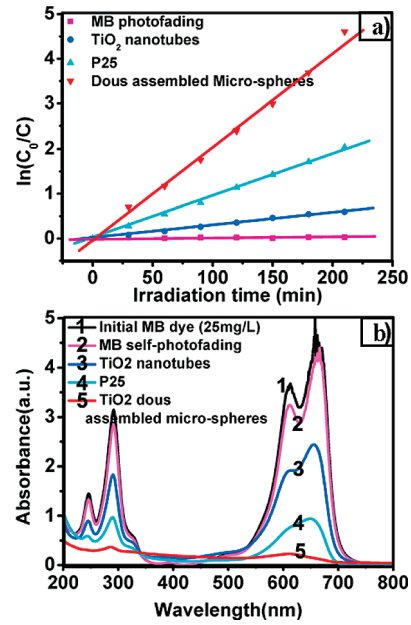

Figure 9. (a) Photocatalytic degradation rates of MB for four photocatalysts versus logarithms of normalized dye concentrations. (b) UV−vis absorption spectra of the MB degraded by different photocatalysts for 210 min under UV irradiation.

3.3. The Photocatalytic Activity. In order to demonstrate the functionality of the as-fabricated TiO_2 dous assembled microspheres, their photocatalytic activity was evaluated based upon the removal of methylene blue (MB) dye in the aqueous solution. For comparison, the photocatalytic activity of the as-fabricated TiO_2 nanotubes and P25 particles were also investigated. First, 30 mg of the TiO_2 microspheres, TiO_2 nanotubes, and P25 particles were respectively immersed into three parts of 100 mL of MB (25 mg L^{-1}) aqueous solutions in dark for 20 h to establish an adsorption/desorption equilibrium of MB on the surfaces of these samples. Subsequently, these samples were separated from the MB aqueous solutions, and added to 15 mL of MB (25 mg L^{-1}) aqueous solutions to conduct the photocatalysis experiments. The ultraviolet light (8 W of power) was used as the UV light source. During the process of photocatalysis experiments, the changes of the concentration of MB were monitored by UV−vis spectroscopy. Figure 9a shows the degradation curves of MB, presented as the logarithms of the time-dependent normalized dye concentration, which is the ratio of the initial concentration and the actual dye concentration (C_0/C) at any time for the single-crystalline TiO_2 dous assembled microspheres, the TiO_2 nanotubes, and P25 particles. To the linear shape of the curves we can fit first-order decomposition kinetics.[36] $\ln(C_0/C) = kt$, where k is a pseudofirst-rate kinetic constant and t is the irradiation time. The resulting k values represent a good measure of the overall photodegradation rate. Evidently, the pseudo-first-rate kinetic constant of the photocatalytic degradation of MB with the assistance of the single-crystalline TiO_2 dous assembled microspheres is significantly higher than that of MB self-photofading and the other photocatalysts (TiO_2 nanotubes and P25 particles). MB dye was almost completely removed after 210 min, as shown in Figure 9b.

4. Conclusions

In conclusion, unique structural single-crystalline anatase TiO_2 dous assembled microspheres were created by transforming the

TiO_2 nanotubes under hydrothermal reaction conditions. Then detailed structural analysis was carried out. The opening and hollow dous expose one {001} face with high surface energy and eight {101} faces with relatively low surface energy, and display excellent photocatalytic activity. Moreover, the interesting geometries might also result in the improvement of the properties for applications in solar cells, photonic and optoelectronic devices, sensors. In addition, the method and mechanism of synthesizing the single-crystalline anatase TiO_2 dous can be exploited in synthesizing the anatase TiO_2 single crystals with special morphologies.

Acknowledgment. This research was supported by National Major Project of Fundamental Research: Nanomaterials and Nanostructures (Grant No. 2005CB623603), National Natural Science Foundations of China (Grant Nos. 90406008, 10674138, and 20571022), and by the Knowledge Innovation Program of the Chinese Academy of Sciences (Grant No. 074N4H1121).

References

(1) Wang, X. D.; Graugnard, E.; King, J. S.; Wang, Z. L.; Summers, C. J. *Nano Lett.* **2004**, *4*, 2223–2226.
(2) Funk, S.; Hokkanen, B.; Burghaus, U.; Ghicov, A.; Schmuki, P. *Nano Lett.* **2007**, *7*, 1091–1094.
(3) Mor, G. K.; Shankar, K.; Paulose, M.; Varghese, O. K.; Grimes, C. A. *Nano Lett.* **2006**, *6*, 215–218.
(4) Park, J. H.; Kim, S.; Bard, A. J. *Nano Lett.* **2006**, *6*, 24–28.
(5) Zhu, K.; Neale, N. R.; Miedaner, A.; Frank, A. J. *Nano Lett.* **2007**, *7*, 69–74.
(6) Ma, R. Z.; Fukuda, K.; Sasaki, T.; Osada, M.; Bando, Y. *J. Phys. Chem. B.* **2005**, *109*, 6210–6214.
(7) Varghese, O. K.; Gong, D.; Paulose, M.; Ong, K. G.; Grimes, C. A. *Sens. Actuator B-Chem.* **2003**, *93*, 338–344.
(8) Bao, S. J.; Li, C. M.; Zang, J. F.; Cui, X. Q.; Qiao, Y.; Guo, J. *Adv. Funct. Mater.* **2008**, *18*, 591–599.
(9) Linsebigler, A. L.; Lu, G. Q.; Yates, J. T. *Chem. Rev.* **1995**, *95*, 735–758.
(10) Asahi, R.; Morikawa, T.; Ohwaki, T.; Aoki, K.; Taga, Y. *Science* **2001**, *293*, 269–271.
(11) Chae, S. Y.; Park, M. K.; Lee, S. K.; Kim, T. Y.; Kim, S. K.; Lee, W. I. *Chem. Mater.* **2003**, *15*, 3326–3331.
(12) Burda, C.; Lou, Y. B.; Chen, X. B.; Samia, A. C. S.; Stout, J.; Gole, J. L. *Nano Lett.* **2003**, *3*, 1049–1051.
(13) Hu, L. H.; Dai, S. Y.; Weng, J.; Xiao, S. F.; Sui, Y. F.; Huang, Y.; Chen, S. H.; Kong, F. T.; Pan, X.; Liang, L. Y.; Wang, K. J. *J. Phys. Chem. B.* **2007**, *111*, 358–362.
(14) Niitsoo, O.; Sarkar, S. K.; Pejoux, C.; Rühle, S.; Cahen, D.; Hodes, G. *J. Photochem. Photobiol., A* **2006**, *181*, 306–313.
(15) Robel, I.; Kuno, M.; Kamat, P. V. *J. Am. Chem. Soc.* **2007**, *129*, 4136–4137.
(16) Yang, H. G.; Sun, C. H.; Qiao, S. Z.; Zou, J.; Liu, G.; Smith, S. C.; Cheng, H. M.; Lu, G. Q. *Nature* **2008**, *453*, 638–642.
(17) Hosono, E.; Fujihara, S.; Lmai, H.; Honma, I.; Masaki, I.; Zhou, H. S. *ACS Nano* **2007**, *1*, 273–278.
(18) Jun, Y. W.; Casula, M. F.; Sim, J. H.; Kim, S. Y. J.; Cheon, A. P.; Alivisatos, *J. Am. Chem. Soc.* **2003**, *125*, 15981–15985.
(19) Barnard, A. S.; Curtiss, L. A. *Nano Lett.* **2005**, *5*, 1261–1266.
(20) Penn, R. L.; Banfield, J. F. *Geochim. Cosmochim. Acta* **1999**, *63*, 1549–1557.
(21) Donnay, J. D. H.; Harker, D. *Am. Mineral.* **1937**, *22*, 446–467.
(22) Lazzeri, M.; Vittadini, A.; Selloni, A. *Phys. Rev. B.* **2001**, *63*, 155409.
(23) Macak, J. M.; Tsuchiya, H.; Taveira, L.; Aldabergerova, S.; Schmuki, P. *Angew. Chem., Int. Ed.* **2005**, *44*, 7463–7465.
(24) Hu, X. Y.; Zhang, T. C.; Jin, Z.; Xu, W.; Yan, J.; Zhang, J. X.; Zhang, J. P.; Zhang, L. D.; Wu, Y. C. *Mater. Lett.* **2008**, *62*, 4579–4581.
(25) Diebold, U. *Surf. Sci. Rep.* **2003**, *48*, 53–229.
(26) Fang, J.; Bi, X. Z.; Si, D. J.; Jiang, Z. Q.; Huang, W. X. *Appl. Surf. Sci.* **2007**, *253*, 8952–8961.
(27) Wang, W. W.; Zhu, Y. J.; Yang, L. X. *Adv. Funct. Mater.* **2007**, *17*, 59–64.
(28) Wang, X.; Yu, L. J.; Hu, P.; Yuan, F. L. *Cryst. Growth Des.* **2007**, *7*, 2415–2418.
(29) Xi, G. C.; Xiong, K.; Zhao, Q. B.; Zhang, R.; Zhang, H. B.; Qian, Y. T. *Cryst. Growth Des.* **2006**, *6*, 577–582.
(30) Yu, J. C.; Xu, A. W.; Zhang, L. Z.; Song, R. Q.; Wu, L. *J. Phys. Chem. B.* **2004**, *108*, 64–70.
(31) Yu, D. B.; Sun, X. Q.; Zou, J. W.; Wang, Z. R.; Wang, F.; Tang, K. *J. Phys. Chem. B* **2006**, *110*, 21667–21671.
(32) Penn, R. L.; Banfield, J. F. *Science* **1998**, *281*, 969–971.
(33) Alivisatos, A. P. *Science* **2000**, *289*, 736–737.
(34) Banfield, J. F.; Welch, S. A.; Zhang, H. Z.; Ebert, T. T.; Penn, R. L. *Science* **2000**, *289*, 751–754.
(35) Chen, M.; Xie, Y.; Lu, J.; Xiong, Y.; Zhang, S.; Qian, Y.; Liu, X. *J. Mater. Chem.* **2002**, *12*, 748–753.
(36) Krýsa, J.; Waldner, G.; Měšťánková, H.; Jirkovský, J.; Grabner, G. *Appl. Catal., B* **2006**, *64*, 290–301.

CG801181Y